Journal of Photochemistry and Photobiology A: Chemistry 204 (2009) 83–89

Contents lists available at ScienceDirect

Journal of Photochemistry and Photobiology A: Chemistry

journal homepage: www.elsevier.com/locate/jphotochem

Chlorophyll-based photocatalysts and their evaluations for methyl orange photoreduction

Meenal Joshi[a], Sanjay P. Kamble[b], Nitin K. Labhsetwar[a], D.V. Parwate[c], Sadhana S. Rayalu[a,*]

[a] Environmental Material Unit, National Environmental Engineering Research Institute (NEERI), Nagpur 440 020, India
[b] National Chemical laboratory (NCL), Dr. Homi Bhabha Road, Pune 411 008, India
[c] Rashtrasant Tukadoji Maharaj Nagpur University Nagpur 440010, India

ARTICLE INFO

Article history:
Received 21 April 2008
Received in revised form 17 November 2008
Accepted 27 January 2009
Available online 7 February 2009

Keywords:
Chlorophyll-based photocatalyst
Mesoporous material
Methyl orange
Photoreduction

ABSTRACT

Immobilization of chlorophyll on different functionalized mesoporous materials has been attempted. The replacement of butanediol with monoethanol amine has resulted in increase in chlorophyll loading by a factor of two. The maximum immobilization of chlorophyll was on MCM-41 functionalized with monoethanolamine MCM-41/MEA/Chl) as compared to other mesoporous materials. This material has been characterized using XRD, UV–vis diffuse reflectance spectroscopy, scanning electron microscopy (SEM-EDX) and fluorescence spectroscopy. The photocatalytic reduction of methyl orange (MO) was studied using MCM-41/MEA/Chl as photocatalyst under the visible light. The photocatalytic reduction of MO was 0.396 mg/g of MCM-41/MEA/Chl photocatalyst as compared to 0.508 mg/g of TiO_2 for that of Degussa P-25 photocatalyst. The effect of various operating parameters like catalyst loading, initial concentration and intensity of light has also been studied. Photocatalytic property of chlorophyll-based photocatalytic material indicates that chlorophyll acts as a reaction center, which absorbs visible light and generates electron, which is transferred to different electron acceptors reducing MO into derivative of hydrazine.

1. Introduction

Many inorganic photocatalysts have been reported, such as TiO_2, CdS and SiC, for various applications including dye degradation and water splitting [1,2]. Titanium dioxide is widely used photocatalyst, which is active mainly in UV range. It is therefore imperative to develop photocatalytic material that can work in visible range of electromagnetic spectrum. This essentially requires development of light harvesting system effective in visible light. Many attempts have been made in this regard [3,4]. In plants, chlorophyll plays similar role during photosynthesis. Photosynthesis in plants comprises of two major reactions, one is light dependent reaction while another is carbon assimilation (dark reaction). During light reaction chlorophyll and other accessory pigments harvest light energy, and conserve it as ATP and NADPH.

The structure of chlorophyll (Fig. 1) comprises of four pyrrole rings linked together by intermediate atomic groups. Each ring bears side chains. Magnesium lies in the center of the structure. Among the side chains, the most predominant side chain is phytol. It makes up about one-third of the chlorophyll molecule. It has a strong affinity for oxygen and may be responsible for reducing action of chlorophyll [5].

The chlorophyllous pigments are unstable in organic solutions but when these pigments are adsorbed on solid support, the degree of denaturation decreases effectively [6]. It is therefore essential to immobilize chlorophyll on a suitable substrate. Various mesoporous materials such as folded sheet materials, mesoporous silica have been reported for effective inclusion of chlorophyllous pigments [7–10]. Mesoporous materials are good hosts for chlorophyllous pigments as they have large surface area with effective pore diameter. Functionalization and surface modification of solid support suppresses the denaturation of chlorophyll effectively.

MCM-41 is a member of M41S family with hexagonal arrays of uniform pore size (pore diameter in a range 15–100 Å) [11]. Functionalization of mesoporous materials with α–ω diol has been reported [3]. In the present study, we have tried to functionalize silica gel, meso-alumina, meso-titania and MCM-41 with monoethanolamine (MEA). The functionalized matrices were then used for incorporation of chlorophyll and subsequently studied for its photocatalytic properties towards reduction of methyl orange (MO). Photoreduction of MO has been used as a diagnostic tool for assessing photo reduction property of these photocatalysts. [12]. The selected chlorophyll-based photocatalytic material was studied for various operating parameters like catalyst loading, initial concentration and illumination intensity.

* Corresponding author. Fax: +91 712 2249900.
E-mail address: s_rayalu@neeri.res.in (S.S. Rayalu).

1010-6030/$ – see front matter © 2009 Elsevier B.V. All rights reserved.
doi:10.1016/j.jphotochem.2009.01.016

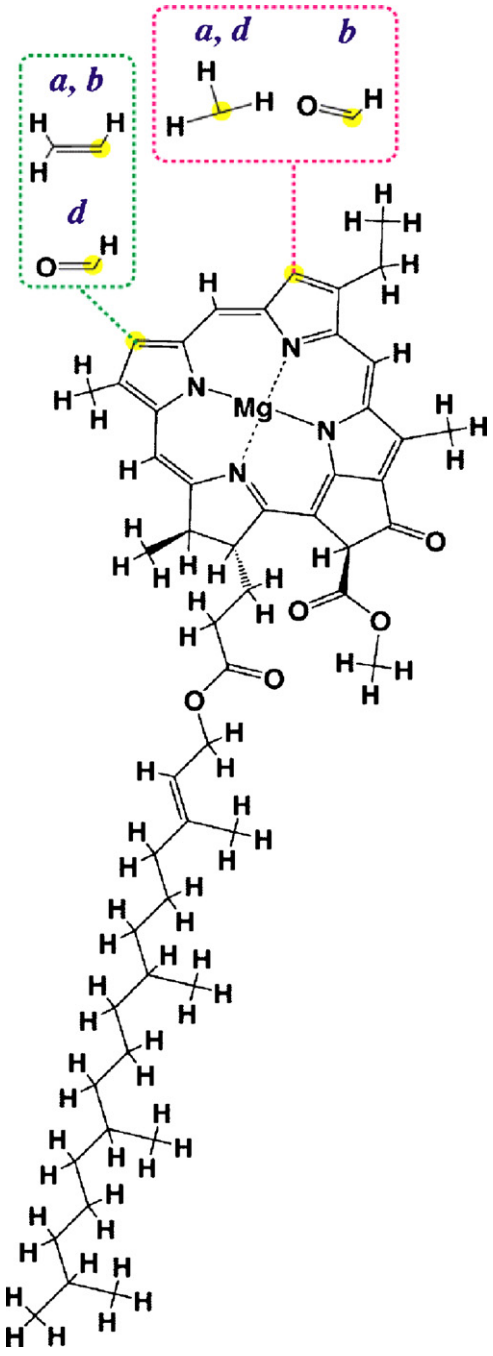

Fig. 1. Structure of chlorophyll.

2. Experimental

2.1. Materials

The chemicals used in the synthesis were hexadecyl trimethyl ammonium bromide (HDTMA-Br) silica gel, monoethanolamine, ethanol, sucrose, sodium chloride, acetone, acetic acid, methyl orange, aluminium nitrate (Merck, India Ltd.), fumed silica (BDH, Germany) and tetra methyl ammonium hydroxide (TMAOH) (Loba Chemicals, India). Spinach was procured from the local market in Nagpur, for extraction of chlorophyll. All chemicals used were of purest research grade available. The 100, 200 and 400 W tungsten lamps were procured from Philip India Ltd., Mumbai. Chitosan was procured from Chemchito India Ltd., Chennai.

2.2. Synthesis of materials

The synthesis of composite photocatalyst involves following steps:

I. Synthesis of bare matrices and its functionalization.
II. Extraction of chlorophyll.
III. Immobilization of chlorophyll on functionalized matrices.

Commercially available silica gel was used for chlorophyll incorporation, while meso alumina (chitosan-based), meso titania (chitosan-based), MCM-41 matrices were synthesized and functionalized as follows.

2.2.1. Synthesis of bare matrices and its functionalization

2.2.1.1. Synthesis of meso-alumina (chitosan-based). 9 g of chitosan was added in 300 mL of 5% acetic acid and stirred for 1 h. Aluminum nitrate solution (27.6 g aluminum nitrate dissolved in 120 mL distilled water) was added to chitosan solution and stirred further for 3 h. Alumina–chitosan solution was added drop wise into 400 mL 50% ammonia solution under constant stirring. This resulted in the formation of gel macrospheres. These macrospheres were stabilized in ammonia solution for 1 h (without stirring) and subsequently washed repeatedly with distilled water. Macrospheres were dried at ambient temperature for 24 h and calcined at 550 °C for 5 h [13].

2.2.1.2. Synthesis of meso-titania (chitosan-based). The meso-titania was synthesized similarly as mesoalumina replacing alumina precursor with titania (titanium isopropoxide).

2.2.1.3. Synthesis of MCM-41. 9.84 g of hexadecyl trimethyl ammonium bromide (HDTMA-Br) was mixed with 67 mL of water and stirred for 5 min. Tetra methyl ammonium hydroxide (TMAOH) was added drop wise in the above mixture and stirred for 10 min. 6 g of fumed silica was added slowly and stirring was continued for 1.5 h. The mixture was crystallized at 110 °C for 48 h in an autoclave. Crystallized product was dried at 60 °C and calcined at 550 °C for 6 h to obtain the final product [11].

2.2.1.4. Functionalization of bare matrices. 1 g of each of different matrices was mixed with 10 mL of MEA in 50 mL ethanol solution. It was then refluxed for 2 h at 80°C and the resultant mass was filtered and dried at 60 °C for 3 h.

2.2.2. Extraction of chlorophyll from spinach

Fresh spinach leaves free from midrib were ground with 0.25 M sucrose solution in saline. Then the spinach leaves extract was filtered through glass wool. Filtered extract was centrifuged at 10,000 rpm for 5 min and supernatant was again centrifuged for 10 min at 5000 rpm. The green coloured pellet of chlorophyll was obtained, which was suspended in 90% acetone solution. P.R. Gorham described the extraction of chlorophyll from spinach similarly [14]. Chlorophyll concentration after extraction from spinach is 109.33 mg of chlorophyll per 100 g of spinach

2.2.3. Immobilization of chlorophyll on functionalized matrices

1 g of functionalized matrix was mixed with 75 mL of chlorophyll solution (Initial chlorophyll solution). This mixture was stirred for 2 h. It was centrifuged at 5000 rpm for 10 min. Adsorption cycle was repeated thrice. The immobilization was higher in the first cycle and gradually shows saturation in the subsequent cycles. Supernatant was analyzed spectrophotometrically at wavelengths 630, 647, 663 and 750 nm [15]. The amount of chlorophyll adsorbed was calculated from the difference between the initial chlorophyll concentration and final chlorophyll (after adsorption on matrix)

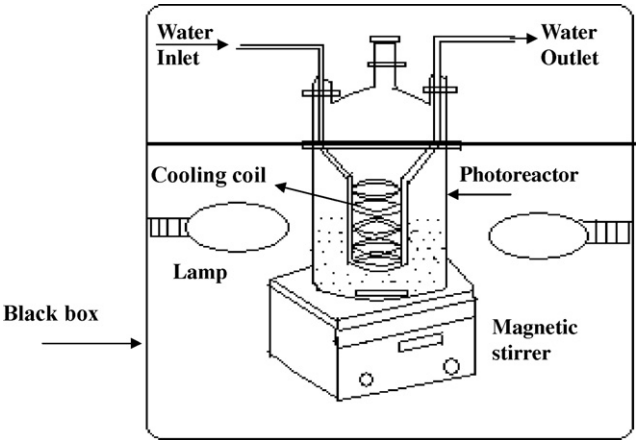

Fig. 2. Schematic diagram of photo reactor.

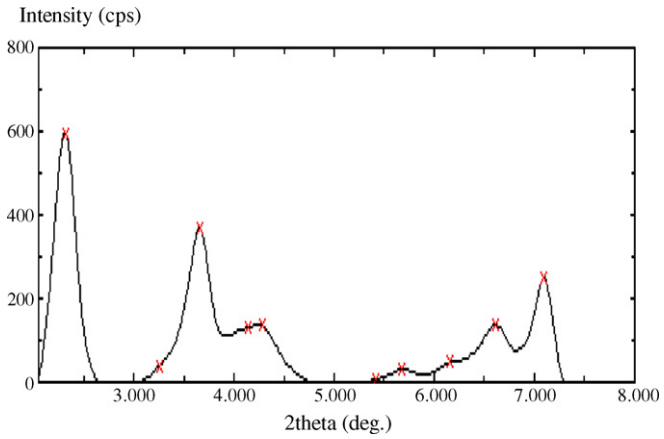

Fig. 3. XRD pattern of MCM-41.

concentration. The ratio of chlorophyll to matrix was calculated thereafter as mg of chlorophyll per g of catalyst.

2.3. Characterization of chlorophyll-based photocatalysts

X-ray diffraction patterns for MCM-41 was obtained on Rigaku Miniflex II, Desktop X-ray diffractometer with Cu Kα radiations. UV–vis diffuse reflectance spectra (UV-DRS) were obtained on PerkinElmer Lambda 900 spectrophotometer equipped with an integrated sphere, $BaSO_4$ was used as a reference material. Scanning electron microscopic (SEM-EDX) images were obtained on JEOL JXA-840A electron probe microanalyser. Fluorescence of chlorophyll conjugate and chlorophyll in 90% acetone was obtained using fluorescence spectrophotometer Hitachi F4500. Absorbance spectra were measured using PerkinElmer Lambda 900 spectrophotometer.

2.4. Experimental method for reduction of methyl orange

Photoreduction of MO was carried out in a three neck borosilicate glass reactor having volume of 50 cm^3 equipped with cooling coil. The temperature of the reaction mixture was maintained at near ambient temperature (20–25 °C) by passing cold water through the cooling coil. The experimental set up for MO photoreduction is shown in Fig. 2. 10 cm^3 MO solution [prepared in ethanol–water system (1:40)] was placed in the reactor and known amount of photocatalyst was added to it. The reaction mixture was then illuminated using tungsten lamp for 8 h along with constant stirring. During the illumination, sample was shielded from heat by circulation of cold water. After completion of experiment, concentration of irradiated sample was measured spectrophotometrically at a wavelength of 464 nm as described in previous studies by the authors [12]. The percentage of MO reduction was calculated by the difference between initial and the final concentrations of the samples. The effect of different factors like the adsorption effect and filtration effect were taken into consideration during the MO reduction calculations.

3. Results and discussion

Functionalization of matrices plays an important role to make them suitable for immobilization of chlorophyll. This is because bare matrices can possess acidic sites, which may cause denaturation of chlorophyll, i.e. conversion of chlorophyll into pheophytine. To eliminate such a possibility, the functionalization of matrices with basic compound such as MEA was attempted. The stability of photocatalyst sample has been confirmed using various instrumental techniques including UV-DRS, fluorescence spectroscopy etc.

3.1. Characterization of materials

The crystallinity of MCM-41 was observed from X ray diffractogram (Fig. 3). The distinct peaks at 2θ values equal to 2.3°, 3.6°, 4.2°, 7.1° corresponds to $h\,k\,l$ reflection planes 1 0 0, 1 1 0, 2 0 0 and 2 1 0, respectively. These values indicate the long-range ordered mesoporous structure [16].

The diffused reflectance UV–vis spectrum for chlorophyll in 90% acetone and MCM-41/MEA/Chl is shown in Fig. 4. The absorption maxima can be seen at 418 and 669 nm, which confirm that the composite photocatalyst is active in visible range.

Fluorescence emission spectra of chlorophyll in 90% acetone and MCM-41/MEA/chl photocatalyst are presented in Fig. 5. The excitation wavelength for chlorophyll in 90% acetone as reported in the literature is 470 nm with the corresponding emission peak of at 650 nm. The emission peak for chlorophyll immobilized on MCM-41/MEA was observed at 664 nm, which indicates that chlorophyll retained its activity after immobilization.

SEM-EDX analysis of MCM-41/MEA/Chl is given in Fig. 6. Magnesium percentage is 0.51 mass percent. This confirms the presence of chlorophyll moiety in the synthesized photocatalyst.

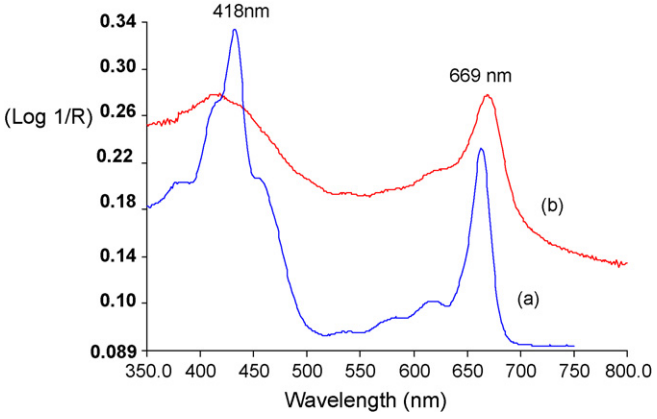

Fig. 4. Diffuse reflectance spectra of (a) chlorophyll in 90% acetone and (b) chlorophyll adsorbed on MCM-41/MEA.

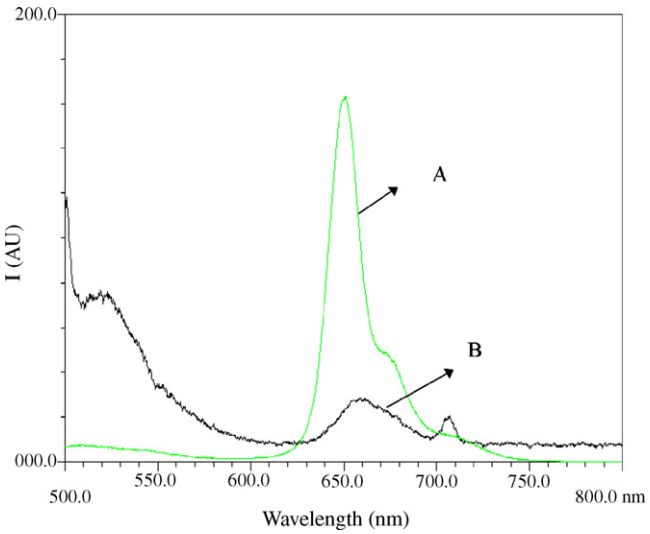

Fig. 5. Fluorescence emission spectra of (A) chlorophyll in 90% acetone and (B) chlorophyll adsorbed on MCM-41/MEA.

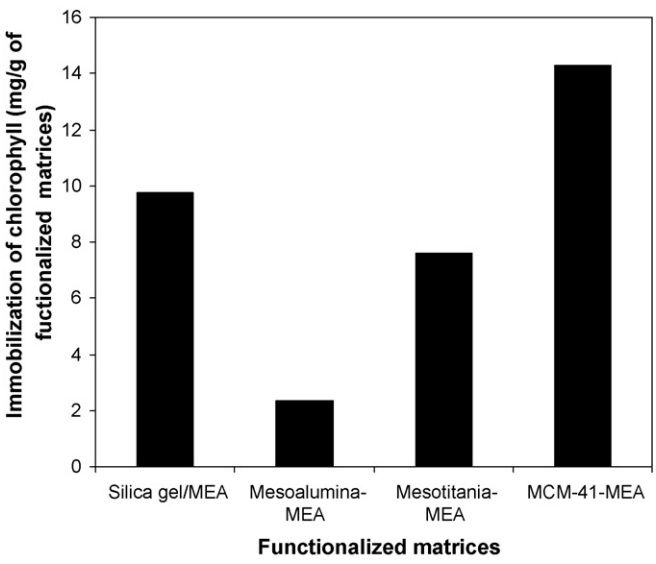

Fig. 7. Immobilization of chlorophyll on different functionalized matrices.

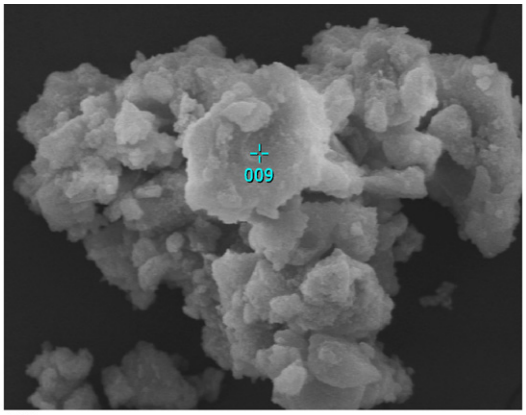

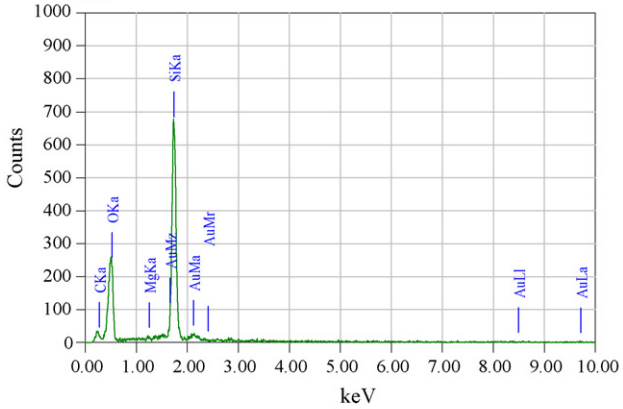

ZAF Method Standardless Quantitative Analysis
Fitting Coefficient : 0.3218

Element	(keV)	mass%	Error%	At%	Compound	mass% Cation	K
C K	0.277	11.69	0.41	19.74			1.7345
O K	0.525	34.35	0.33	43.55			34.5152
Mg K	1.253	0.51	0.20	0.42			0.5046
Si K	1.739	49.71	0.23	35.90			60.6584
Au M	2.121	3.74	1.28	0.39			2.5873
Total		100.00		100.00			

Fig. 6. SEM-EDX image of MCM-41/MEA/Chl.

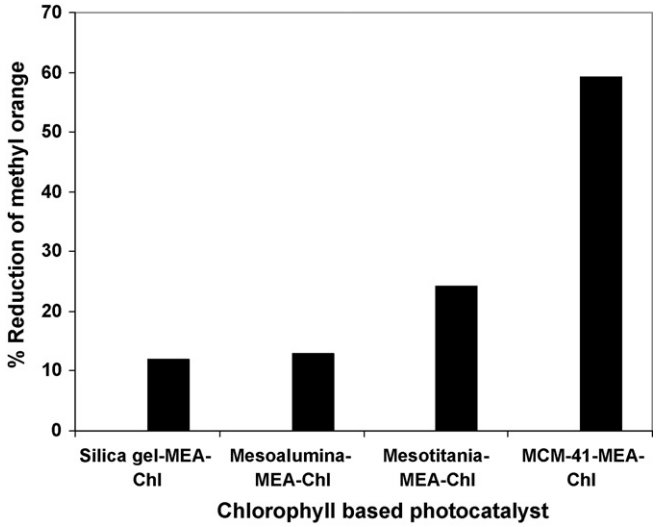

Fig. 8. Comparison of MO photoreduction by various chlorophyll-based photocatalysts.

3.2. Effect of matrices on photocatalytic reduction of MO

The chlorophyll was incorporated on different functionalized matrices namely silica gel/MEA, meso-alumina/MEA, mesotitania/MEA and MCM-41/MEA. The loadings of chlorophyll on different matrices are shown Fig. 7. This figure shows that the immobilization of chlorophyll on MCM-41/MEA (14.30 mg/g) was highest followed by silica gel/MEA (9.77 mg/g), mesotitania/MEA (7.59 mg/g), and mesoalumina/MEA (2.34 mg/g).

All the chlorophyll-based photocatalysts were evaluated for MO photoreduction (Fig. 8). From this figure, it was observed that the MO reduction was highest in case of MCM-41/MEA/Chl as compared to the other chlorophyll-based photocatalyst. Therefore, further detailed studies were restricted to MCM-41/MEA/Chl photocatalyst.

3.3. Photoreduction of methyl orange using MCM-41/MEA/chl photocatalyst

3.3.1. Variation in photoreduction with time

The variation in photoreduction of MO with respect to time was followed using MCM-41/MEA/Chl photocatalyst and is presented in Fig. 9. It was observed that initially the kinetics is very slow up to 240 min. Thereafter the rate of photoreduction increases substantially. After 390 min (6 h and 50 min) there is a sudden increase in photoreduction rate and remains constant up to 8 h. The addition of small quantity of sacrificial donor seems to facilitate the reaction. However, during the course of the reaction the donor is consumed, thus disturbing the electron chain with a consequent effect of reaction termination.

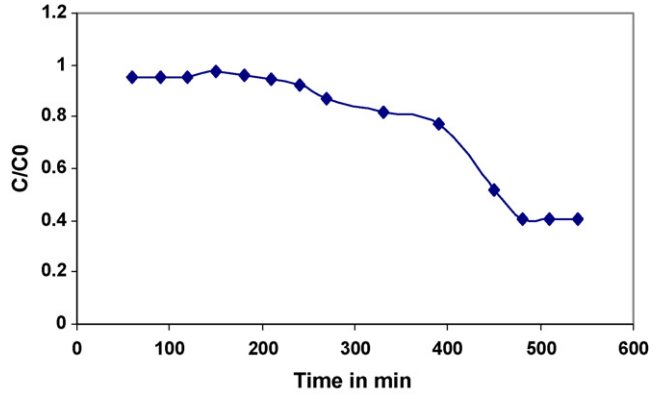

Fig. 9. Variation in MO photoreduction with time using MCM-41/MEA/Chl photocatalyst.

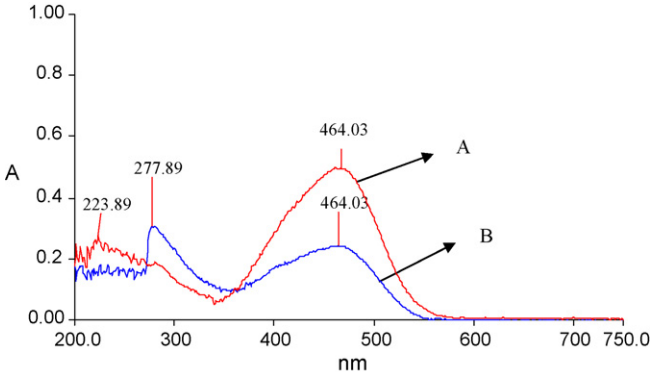

Fig. 10. Adsorption spectra of (A) initial MO solution and (B) after MO photoreduction experiment (photocatalyst loading = 7.5%, w/v).

3.3.2. Effect of catalyst loading

Fig. 10 illustrates the absorption spectrum of photoreduction of MO by MCM-41/MEA/Chl. Fig. 10A gives the absorption spectrum of initial MO solution, which confirms the presence of MO with an absorption maxima at 464 nm. Fig. 10B shows absorption spectrum after photoreduction experiment, which clearly shows the reduction in MO peak area with the formation of new peak at 277 nm. This indicates that the MO concentration decreases with the formation of hydrazine derivative [17]. Fig. 11 shows effect of catalyst dose on MO photoreduction. The MO photoreduction was increased on increasing the catalyst loading upto 7.5% (w/v). Further increase of catalyst loading results in substantial decrease in photoreduction activity. This is because as the catalyst loading is increased, there is an increase in the surface area of the catalyst available for photoreduction of MO. But increase in the catalyst loading increases the solution opacity, leading to decrease in the penetration of the photon flux in the reactor and thereby decreasing the overall photocatalytic reduction rate. Therefore 7.5% (w/v) catalyst loading was used as optimum dose for further experimental studies.

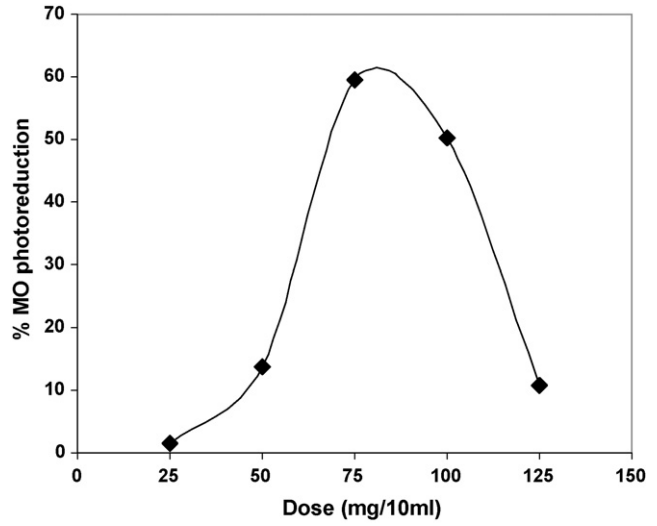

Fig. 11. Effect of photocatalyst loading on MO photoreduction (initial MO concentration – 5 mg/L, illumination intensity – 2.06×10^2 mW/cm^2, and time duration – 8 h).

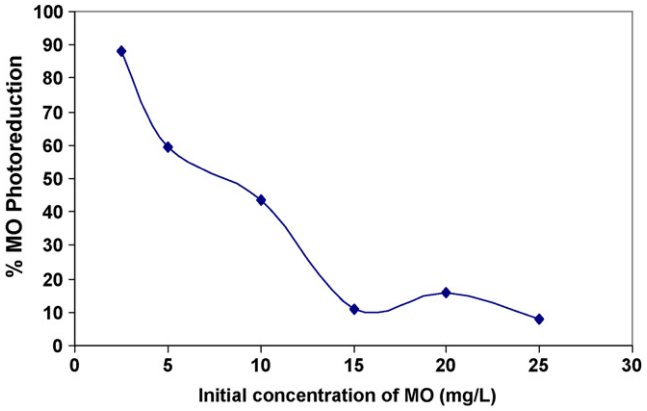

Fig. 12. Effect of initial of methyl orange concentration on photoreduction (photocatalyst loading – 7.5% (w/v), illumination intensity – 2.06×10^2 mW/cm^2, and time duration – 8 h).

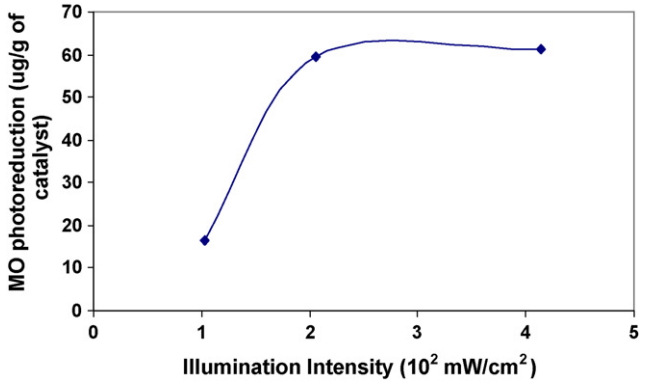

Fig. 13. Effect of illumination intensity variation (initial MO concentration = 5 mg/L, photocatalyst loading = 7.5% (w/v), time duration = 8 h).

3.3.3. *Effect of initial concentration*

The effect of initial concentration on photocatalytic reduction of MO was shown in Fig. 12. It was observed that the reduction of MO was 29.7, 43.8, 17.70, 15.64 and 7.82 μg/g of photocatalyst for initial concentrations of 5, 10, 15, 20 and 25 mg/L, respectively. For concentration variation study the other two parameters were kept constant i.e. loading of photocatalyst (7.5%, w/v) and illumination intensity (2.06×10^2 mW/cm^2). As the catalyst dose and illumination intensity is maintained constant the number of photons, active sites available remain constant. Therefore with increase in MO molecules for same number of active sites and intensity of light, there is a decrease in percent reduction rate. At lower concentrations like 2.5 mg/L the reduction rate increases up to 88% (22 μg/g of photocatalyst).

3.3.4. *Effect of illumination intensity*

Fig. 13 shows the effect of light intensity (1.03×10^2, 2.06×10^2, and 4.13×10^2 mW/cm^2) on photocatalytic reduction of MO. The increase in light input from 1.03×10^2 mW/cm^2 to 2.06×10^2 mW/cm^2 results in increase in reduction of MO, while further increase in light input (4.13×10^2 mW/cm^2) does not show significant impact on further reduction of MO.

It is known that the light provides the photons, absorption of which leads to excitation of ground state electron to excited state. With the increase in intensity of light, the availability of photons also increases which results in increased rate of reaction or the reduction property of the photocatalyst. At higher light intensity the rate is independent of intensity of light and hence further increase in lamp input (4.13×10^2 mW/cm^2) the reduction did not increase much [18].

4. The possible mechanism for the photoreduction MO using MCM-41/MEA/Chl

The possible mechanism for the photoreduction using MCM-41/MEA/Chl could be as follows:

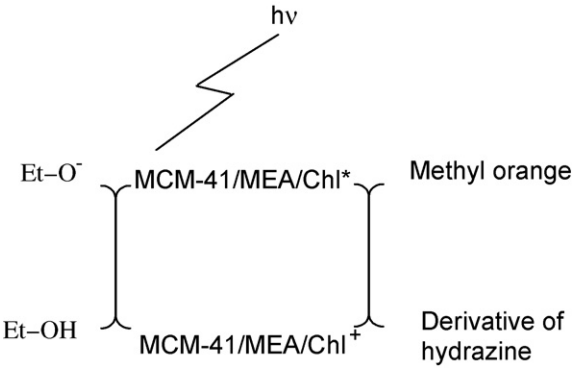

(i) Chlorophyll present in the catalyst absorbs light and gets converted in to excited complex (MCM-41/MEA/Chl*).
(ii) Excited chlorophyll complex releases electron and gets converted into cationic form (MCM-41/MEA/Chl$^+$).
(iii) The released electron is now available for reduction of MO.
(iv) During the reduction process MO is converted to hydrazine derivative. Ethanol present in the solution provides electron to cationic form to reproduce MCM-41/MEA/Chl.

5. Conclusions

Chlorophyll has been successfully immobilized on four different mesoporous matrices functionalized with monoethanolamine. The MCM-41/MEA matrix shows highest chlorophyll immobilization as compared to other mesoporous matrices used after functionalization with monoethanolamine. The denaturation of chlorophyll is suppressed due to functionalization of matrices. The absorption maxima observed for the chlorophyll conjugate are 418 and 669 nm, which suggest that the conjugate is active in visible region. Chlorophyll conjugate appears to be quite photo-active as it can reduce MO effectively (0.396 mg/g of catalyst). Effects of various operating parameters on photocatalytic reduction of MO were studied. It was observed that the operating conditions such as catalyst loading, initial concentration of MO and intensity of light has significant effect on MO photoreduction. This confirms that chlorophyll conjugate can work as good photocatalyst; its activity can be further improved by increasing the chlorophyll concentration on host material and such studies are under progress to eventually biomimic the natural process of chlorophyll-based photocatalytic activity.

Acknowledgements

Financial support from the Department of Science and Technology (DST) Govt. of India is gratefully acknowledged. We are thankful to Dr. G.L Bodhe, Dr. V.M. Shinde and Dr. L. N. Sangolkar (NEERI) for their co-operation during various evaluations and characterizations. The authors also thankfully acknowledge the constant encouragement and support from Director, NEERI, Nagpur.

References

[1] J. Oudenhoven, F. Scheijen, M. Wolfs, H. Niemantsverdriet, Chem. Catal. Syst. 2 (2004) 1–22.
[2] N. Serpone, A.V. Emeline, Int. J. Photo Energy 4 (2002) 91–131.

[3] M. Ni, K.H. Michael Leung, Y.C. Dennis Leung, K. Sumathy, Renewable Sustainable Energy Rev. 11 (2005) 1–26.
[4] X. Chen, S.S. Mao, Chem. Rev. 107 (2007) 2891–2959.
[5] B.S. Mayer, D.B. Anderson, Plant Physiol. (1940) 305–314.
[6] S. Murata, H. Furukawa, K. Kuroda, Chem. Mater. 13 (2001) 2722–2729.
[7] T. Itoh, K. Yano, Y. Inade, Y. Fukushima, J. Mater. Chem. 12 (2002) 3275–3277.
[8] S. Muruta, H. Hata, T. Kimura, Y. Sugahara, K. Kuroda, Am. Chem. Soc. 16 (2000) 7106–7108.
[9] T. Itoh, K. Yano, T. Kajino, S. Itoh, Y. Shibata, H. Mino, R. Miyamoto, Y. Inada, S. Iwai, Y. Fukushima, J. Phys. Chem. 108 (2004) 13683–13687.
[10] T. Itoh, K. Yano, Y. Inade, Y. Fukushima, J. Am. Chem. Soc. 124 (2002) 13437–13441.
[11] J.S. Beck, J.C. Vartuli, W.J. Roth, M.E. Leonowicz, C.T. Kresge, K.D. Schmitt, C.T.W. Chu, D.H. Olson, E.W. Sheppard, S.B. Mc-Cullen, J.B. Higgens, J.L. Schlenker, J. Am. Chem. Soc. 114 (1992) 10834–10843.
[12] N. Dubey, S.S. Rayalu, N.K. Labhsetwar, R.R. Naidu, R.V. Chatti, S. Devotta, Appl. Catal. 303 (2006) 152–157.
[13] H.V. Fajardo, A.O. Martins, R.M. Almeida, Mater. Lett. 59 (2005) 3963–3967.
[14] S.P. Colowick, N.O. Kaplan, Methods in Enzymology, vol. I, Academic Press (1955) 19–25.
[15] A. E. Greenberg, R.R. Trussel, E.S. Clesceri, Standard methods for the examination of water and waste water. American Public Health Association (1985) 1067–1070.
[16] C.T. Kresge, M.E. Leonowicz, W.J. Roth, J.C. Vartuli, J.S. Beck, Nature 359 (1992) 710–712.
[17] S. Anandan, M. Yoon, J. Photochem. Photobiol. C: Photochem. Rev. 4 (2003) 5–18.
[18] D.F. Ollis, E. Pelizzetti, N. Serpone, Environ. Sci. Technol. 25 (9) (1991) 1522–1529.